

Contents lists available at [ScienceDirect](http://ScienceDirect.com)

Chemical Engineering Science: X

journal homepage: www.elsevier.com/locate/cesx

The effect of particle properties and solids concentration on the yield stress behaviour of drilling fluid filter cakes

Nikzad Falahati^a, Alexander F. Routh^{a,*}, Kuhan Chellappah^b^a Department of Chemical Engineering and Biotechnology, University of Cambridge, Philippa Fawcett Drive, CB3 0AS Cambridge, UK^b BP plc, Sunbury, London, UK

ARTICLE INFO

Article history:

Received 25 October 2019

Received in revised form 10 February 2020

Accepted 1 March 2020

Keywords:

Filter cake

Porosity

Yield stress

Particle size distribution

Drilling fluid

ABSTRACT

Filter cakes made from model water-based drilling fluids were tested to determine cake properties such as porosity, thickness and yield stress. The effects of drilling fluid particle concentration, size distribution and shape on the properties of the resulting cakes were investigated. A hole punch tester was used to find the shear stress of the cakes, obtaining a yield stress from the measured peak force. The cake yield stress increased with increasing barite solids content in the fluid from 16.5 kPa at 3.1 vol% to 65.6 kPa at 24.8 vol%. A similar trend was observed for cakes made from calcium carbonate. Furthermore, the calcium carbonate cakes were thicker and stronger than the barite equivalents, with yield stresses increasing by between 29% and 56%. The addition of calcium carbonate particles to the existing barite network did not affect the cake thickness appreciably but gave cakes of lower porosity and higher yield stress.

© 2020 The Authors. Published by Elsevier Ltd. This is an open access article under the CC BY-NC-ND license (<http://creativecommons.org/licenses/by-nc-nd/4.0/>).

1. Introduction

Cake filtration occurs inherently in many in situ hydrocarbon reservoir exploitation processes (Civan, 2015). For instance, as fresh rock surface is exposed during overbalanced drilling (the wellbore pressure is higher than the fluid pressure in the rock pores), the drilling fluid tends to permeate into the rock whilst particulates build up on the rock surfaces to form a filter cake. Properties of this cake largely depend on the pressure gradient driving its growth, drilling fluid properties and the rock's porous structure. Ideally, drilling fluid filter cakes should form rapidly and be of low permeability, thin and tough (Bailey et al., 1998). Low permeability cakes protect the rock formation from excessive invasion of drilling fluids, which can impair the formation's permeability and subsequently hydrocarbon production. Thick cakes can lead to excessive torque when rotating the drill-string, excessive drag when pulling it, and lead to other issues such as differential sticking (Fisher et al., 2000).

During drilling, a weak filter cake can easily lose its integrity and, subsequently, allow drilling fluid invasion into the rock as well as increase the occurrence of wellbore stability issues. A competent filter cake can contribute to so-called wellbore strengthening phenomena whereby the maximum pressure the wellbore can withstand is effectively increased (Guo et al., 2014). Wellbore

strengthening is frequently employed when drilling through weak formations which are susceptible to fracturing during drilling. Cook et al. (2016) claim that the strength of a filter cake is particularly important in determining how effectively it can contribute to wellbore strengthening. This claim is backed up by experimental data from Guo et al. (2014).

The integrity of a filter cake across a reservoir is critical for different reasons once a reservoir section is drilled and preparations are being made to produce hydrocarbons; here the function of a filter cake as a barrier to flow is no longer desirable. This is particularly significant for open-hole completions where the operator does not have the option of, for instance, perforating past the near-wellbore region. In this case, filter cake failure is generally induced chemically (e.g. the use of breaker fluids), mechanically (e.g. using scrapers), or hydrodynamically (e.g. by back flow). The back-flow procedure is perhaps the most convenient. Two failure modes during backflow include the formation of pin-holes in the filter cake (erosion channels through which flow can be achieved) or detachment of large slabs of cake from the rock surface. The latter mode can result in undesirable plugging of the completion (e.g. slotted liner or gravel pack) (Cerasi et al., 2001). Which failure mode is likely to dominate is therefore a significant consideration during the design of drilling fluids and completion strategies, and will depend to a large extent on the strength of the filter cake.

Although some researchers have developed techniques to characterise filter cake strength (Zamora, Lai and Dzialowski, 1990; Bailey et al., 1998; Cerasi et al., 2001; Tan and Amanullah, 2001;

* Corresponding author.

E-mail address: afr10@cam.ac.uk (A.F. Routh).

Cook et al., 2016), in general, research involving direct measurements of cake strength has been relatively scarce considering its significance. For practical purposes, the strength of a filter cake is often characterised by its shear yield stress. This quantity is conceptually identical to the shear yield stress commonly used to describe drilling fluids (Bailey et al., 1998), although the fluids tend to give lower yield stress values than their resulting filter cakes; this is not surprising considering a filter cake is essentially a concentrated (with regards to solids content) drilling fluid. From cake strength tests, either an elastic or viscous response is expected from the stress-strain relationship, with a critical stress at the yield point. Filter cakes predominantly behave as elastic solids, and the yield stress marks the transition from elastic behaviour, where the cake is considered competent to a plastic flow regime (Cook et al., 2016). Above this stress threshold, the filter cake can be considered to have 'failed'.

Bailey et al. (1998) developed a hole punch test to directly measure the shear failure of filter cakes. The technique directly measures the force required for cake failure so that the yield stress can be determined. Bailey et al. pressed barite weighted bentonite-based drilling fluids at 2000 kPa, whilst varying the barite concentration to manipulate fluid density. Their results exhibited a peak yield strength at a critical barite concentration. Bailey et al. explain this trend by suggesting that below the critical concentration, barite particles behaved as a filler to bolster the bentonite network, increasing its yield stress. However, beyond this critical concentration, there is sufficient barite to form the core load-bearing matrix, and the bentonite-water gel fills the available space. The roles that the barite and bentonite-water fluid serve essentially switch past this critical concentration. Since the cohesive strength of the barite matrix is much lower than that of the bentonite gel it replaces, the yield stress declines.

Bailey et al. (1998) also used their technique to study the effects of particle size on cake yield stress. This was achieved by adding barite and constant volume fractions of different size grades of calcium carbonate to fluids composed of polymer dissolved in water. Their results showed that higher solids loadings led to an increase in yield stress, and that barite weighted filter cakes gave lower yield stress values than correspondingly sized calcium carbonate weighted filter cakes. Furthermore, they found finer particles to form stronger cakes. The coarser particles formed cakes with low cohesive strength and poor fluid loss control. It was suggested that the surface chemistry of the weighting agents, particularly the surface area of the particles, affects the particle interactions, and hence, the measured yield stress.

Similar observations on the effects of solids content and fine particles on cake strength were made by Cerasi et al. (2001) who performed strength tests using a rheometer with a parallel-plate geometry. They performed one series of experiments by increasing the drill solids content while keeping the overall fluid density constant (presumably by decreasing the calcium carbonate particle concentration). Cerasi et al. found the increasing concentration of drill solids, which were finer than the calcium carbonate particles, to increase yield stress. In a second series of experiments, Cerasi et al. increased the drill solids loading keeping the calcium carbonate concentration fixed. In this case, the extent of yield stress variation was less than with the first series of experiments. Based on these findings, Cerasi et al. proposed that the increase of fines in the filter cake had a more significant influence on yield stress than the increased solids loading in the fluid.

In this work, an experimental setup similar to that of Bailey et al. (1998) is used to investigate the effects of drilling fluid particle volume fraction, size distribution and shape on the properties of the resulting filter cakes. In Section 2, the materials employed and methods used to analyse filter cakes are outlined. Typical stress-strain curves obtained using the hole punch test are presented

and the influence of solids volume fraction, shape and size distribution on the cake yield stress are investigated in Section 3. Section 4 explores the relationships between cake properties such as porosity, thickness and yield stress, and the conclusions are in Section 5.

2. Experimental approach

2.1. Materials

Samples were made with typical water-based drilling fluid components. The base fluid remained consistent throughout, but the solid particulate additives were varied. All fluid samples were made up to 400 ml using deionised water, 1.37 g of xanthan gum and 0.4 g of magnesium oxide (to maintain pH 10). Samples containing graded calcium carbonate and/or barite are given in Table 1. Each sample was prepared using the same mixing procedure and conditions, and rheology tests were performed to check for consistency between similar samples. The volume fraction of calcium carbonate particles in SCal samples are equal to the volume fraction of barite particles in SC equivalents. Medium-sized calcium carbonate particles were further graded into the size ranges using a column of sieves on a mechanical shaker. These sieved size ranges were then used to control the proportion of fine and coarse particles in the blended ratio samples (B1X and B2X): as the number after the 'X' in the sample name increases, the proportion of coarser particles in the sample increases. The total volume fraction of calcium carbonate in each blended ratio sample was kept the same.

Samples with particles of varying shape were made using solid particles with the same solids volume fraction (6.2 vol%) as in SC2; these particles were calcium carbonate (SCal2), talc (Stal), cellulose microcrystalline (Scell) and glass spheres (Sglass). The circularity, defined as the circumference of the equivalent area circle divided by the actual perimeter of the particle, of these particles are given in Table 2.

The components were sequentially added to the water-based fluid and stirred at 6000 RPM using a Silverson Laboratory Mixer with a total mixing time of 35 min. The mixing time was long enough to ensure that the components were homogeneously mixed into the fluid, but short enough to avoid excess heating. A general-purpose mixing head was used on the Silverson to avoid particle size reduction. Particle size distributions were determined using a Malvern Mastersizer 2000, with the data shown in Fig. 1. Particle sizes and circularities (both in Table 2) for the particles used to test the effect of particle shape were measured in the dry state and obtained using a Morphologi G3 Microscope.

2.2. Analysis of filter cakes

Filter cakes were made using an API filter press (Fig. 2) at a constant pressure of 690 kPa for 30 min using a 0.45 μm rated nylon membrane. After an experiment, the filter press was dismantled and the cake was removed with the membrane and sealed in a petri dish to avoid drying. The sample removal was performed carefully to avoid excess fluid on the top of the cake surface and to ensure the cake structure was not disrupted. Three separate filter cake samples were made for each fluid composition tested: one is weighed and left to dry to obtain the porosity, another is placed on the texture analyser to measure thickness and the last is placed on the hole punch platform, which is attached to the texture analyser, to measure mechanical properties.

The most common method to determine filter cake porosity without requiring complicated and expensive equipment (Shirato et al., 1971; Shen, Russel and Auzeais, 1994; Tiller, Hsyung and Cong, 1995; La Heij et al., 1996; Hall et al., 2001; Sedin, Johansson and Theliander, 2003) is to measure the wet cake mass,

Table 1
Fluid compositions for varying barite and calcium carbonate concentration, and, varying particle size distribution samples.

Sample	Barite (vol%)	Calcium carbonate (vol%)				Sieved calcium carbonate (vol%)					
		Ultra-fine	Fine	Medium	Coarse	20–38 μm	38–53 μm	53–63 μm	63–75 μm	75–108 μm	108–150 μm
SC1	3.1	–	–	–	–	–	–	–	–	–	–
SC2	6.2	–	–	–	–	–	–	–	–	–	–
SC3	12.4	–	–	–	–	–	–	–	–	–	–
SC4	18.6	–	–	–	–	–	–	–	–	–	–
SC5	24.8	–	–	–	–	–	–	–	–	–	–
DB1	6.2	–	–	1.5	1.5	–	–	–	–	–	–
DB2	6.2	–	1.5	–	1.5	–	–	–	–	–	–
DB3	6.2	1.5	–	–	1.5	–	–	–	–	–	–
DB4	6.2	–	1.5	1.5	–	–	–	–	–	–	–
DB5	6.2	1.5	–	1.5	–	–	–	–	–	–	–
DB6	6.2	1.5	1.5	–	–	–	–	–	–	–	–
DB7	6.2	0.7	0.7	0.7	0.7	–	–	–	–	–	–
DB8	6.2	–	1.0	1.0	1.0	–	–	–	–	–	–
DB9	6.2	1.0	1.0	1.0	–	–	–	–	–	–	–
B1X2.0	3.1	–	–	–	–	0.2	0.1	0.1	0.3	0.5	1.7
B1X1.5	3.1	–	–	–	–	0.4	0.2	0.1	0.4	0.5	1.4
B1X1.0	3.1	–	–	–	–	0.7	0.2	0.1	0.4	0.5	1.0
B1X0.5	3.1	–	–	–	–	1.5	0.2	0.1	0.3	0.3	0.5
B2X2.0	6.2	–	–	–	–	0.2	0.1	0.1	0.3	0.5	1.7
B2X1.5	6.2	–	–	–	–	0.4	0.2	0.1	0.4	0.5	1.4
B2X1.0	6.2	–	–	–	–	0.7	0.2	0.1	0.4	0.5	1.0
B2X0.5	6.2	–	–	–	–	1.5	0.2	0.1	0.3	0.3	0.5
SCal1	–	3.1	–	–	–	–	–	–	–	–	–
SCal2	–	6.2	–	–	–	–	–	–	–	–	–
SCal5	–	24.8	–	–	–	–	–	–	–	–	–

Table 2
Properties of the substances used for particle shape analysis.

Substance	Circularity	D50 (μm)
Glass	0.88	12.9
Calcium carbonate	0.82	19.2
Barite	0.81	9.7
Talc	0.71	15.6
Cellulose microcrystalline	0.77	66.5

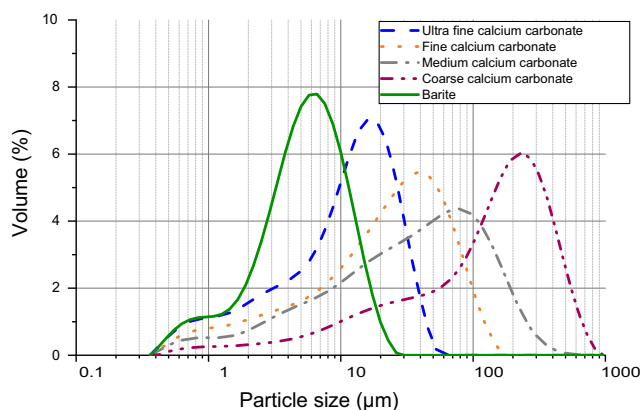


Fig. 1. Particle size distributions of calcium carbonate and barite particles.

then completely dry the cake and measure the dry cake mass (Dewan and Chenevert, 2001; Tien, 2006). However, a challenge often faced with drilling fluid filter cakes is that the suspension/filter cake interface is poorly defined, which then makes it difficult to accurately determine the cake's moisture content. Hence, for this work a method was developed to track the drying rate of the cake over time for detection of when this rate declines significantly. The shift in the mass transfer rate as water is being evaporated from the cake as opposed to the fluid on top of the cake becomes evident in the drying rate curve. As an example, Fig. 2 shows the instantaneous drying rate against drying time, and the point at which the

drying rate experiences a sharp transition can be approximated as the point at which the cake begins to dry. With this approach the liquid content of the cake can be determined, and assuming the void spaces in the filter cake to be saturated with liquid, the porosity is calculated.

Filter cake thickness is an important property as it is required to convert force-displacement data to stress-strain values. With regards to the drilling process, a maximum limit of cake thickness is recommended to avoid problems such as differential sticking of the drill bit. The ability to obtain accurate measurements of the cake thickness is crucial, but, as with the porosity measurements, there are problems with differentiating between the cake and fluid left on the top surface. In this work, cake thickness was determined by using the Texture Analyser's force measurements through the cake sample. A similar method was used by Chen and Hsiau (2009) who used an on-line powder pressure-displacement system to measure the thickness of dust filter cakes. The cake sample is placed on a flat surface below the Texture Analyser probe which is set at a fixed height and approaches the cake at a constant speed, measuring the force as it descends. A force is recorded as soon as the probe contacts the filter cake's top surface and increases further as the probe traverses the cake to approach the bottom surface. The height difference between the top and bottom surfaces is then recorded as the filter cake thickness.

The cake yield stress was found by punching a plunger attached to a Texture Analyser through the cake sample, having carefully peeled off the attached membrane, which sits on top of an opening; see Fig. 2 for images of the test and Fig. 3 for a schematic description. This device, called the hole punch tester, is expected to simulate shear rupture in a simple and inexpensive manner. Bailey et al. (1998), Nandurdikar et al. (2002) and Hao et al. (2016) used a similar hole punch method to carry out cake strength tests. Bailey et al. (1998) compared the yield stress results using this hole punch method to two other techniques: the vane method and the squeeze film method. The hole punch data seemed to correspond well with data from these two other approaches, suggesting it to be a reliable technique. Force-displacement data were obtained with this technique. The shear stress was determined by dividing the force by the cake surface area that is being sheared ($\pi D T$, where D is the open-

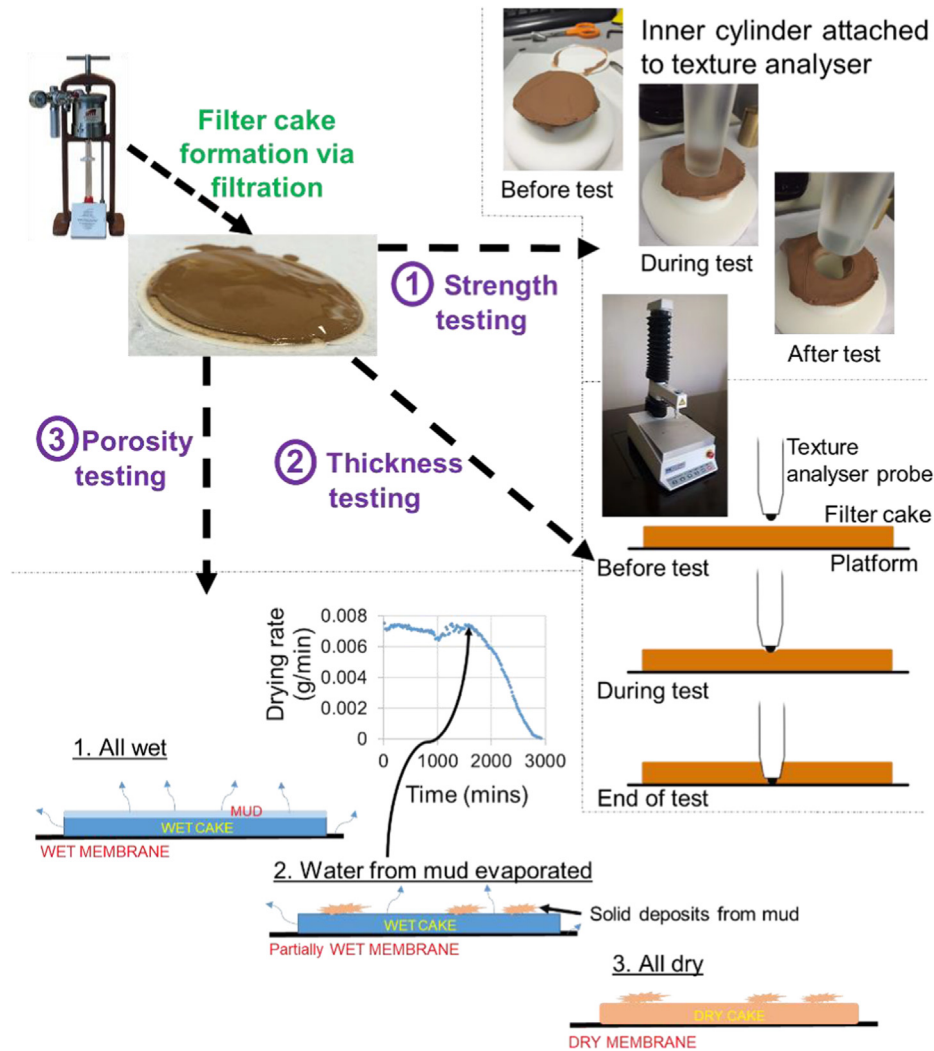


Fig. 2. Summary of experimental procedure showing the tests performed on filter cakes made in the API device.

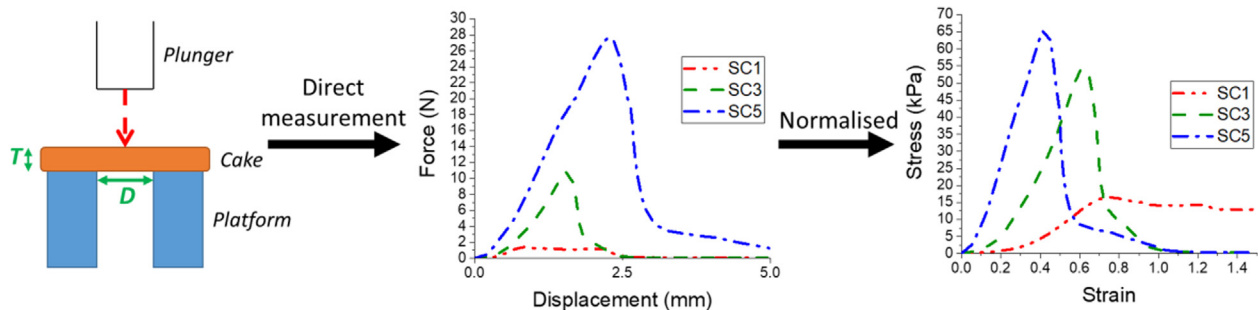


Fig. 3. Schematic of hole punch test and conversion of force-displacement data.

ing diameter and T is the cake thickness), and the strain was calculated by normalising the displacement with the cake thickness. When the peak force is used, the resulting shear stress corresponds to the filter cake's yield stress.

3. Results

3.1. Stress-strain behaviour

Typical stress-strain curves for samples with varying solids volume fraction and particle shape are shown in Figs. 4 and 5. From

Fig. 4, the stress is seen to initially increase linearly as force is applied onto the cake surface. The filter cake undergoes deformation due to this applied load, accounted for via monitoring displacement of the plunger and used to calculate the strain. In the elastic region preceding the critical yield stress, there is an approximately linear relationship between stress and strain, as expected from a predominantly elastic material such as filter cakes. At the yield stress, the integrity of the filter cake is broken and the cake 'fails'. Applying load past this point continues to strain the cake, but the structure can no longer sustain the applied stress. The shape of the curve after the yield point may also be influenced

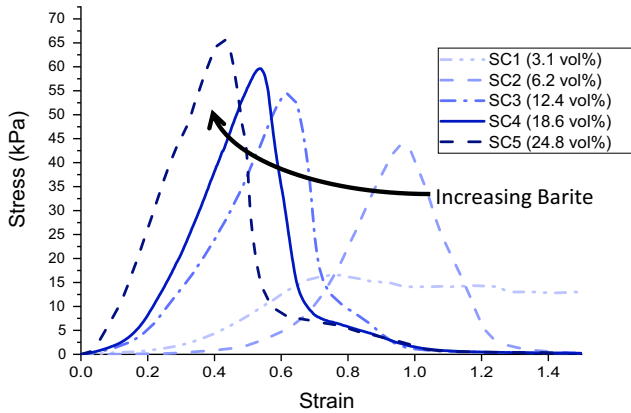


Fig. 4. Stress-strain curves for samples with varying barite compositions.

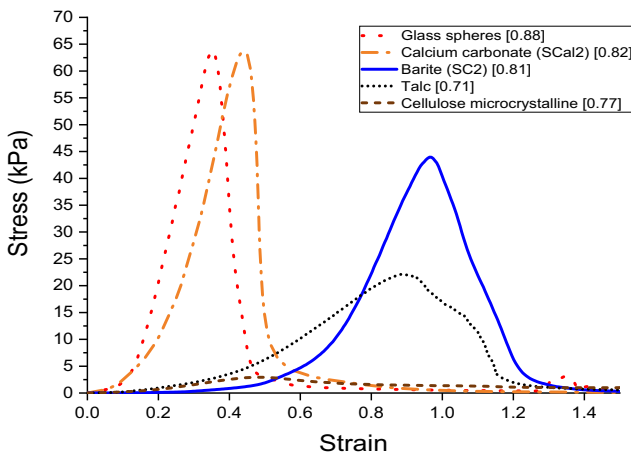


Fig. 5. Stress-strain curves for samples that have varying particle shape; the number inside square brackets in the legend is the circularity of each particle.

by friction with the walls, as the plunger forces cake material into the opening.

Fig. 5 shows that the particles with the highest circularity, glass spheres and calcium carbonate, produce cakes with stress-strain curves that have the steepest gradients. This suggests that these cakes are more resistant to being strained. The cakes made from lower circularity particles have more gradual stress-strain curves up to the yield stress. For barite and talc particles, the strain at which these cakes yield is significantly higher at 0.96 and 0.88, than with the more spherical base particles.

3.2. Varying solids volume fraction

In Fig. 4, from a barite solids loading of 6.2–24.8 vol%, the strain at which the cake fails decreases from 0.96 to 0.42. Also noted is that the yield stress increases with increasing solids content in the fluid; from a yield stress of 16.5 kPa at 3.1 vol% to 65.6 kPa at 24.8 vol%. The effects of varying the solids volume fraction in the fluid on the cake yield stress is illustrated in Fig. 6. The yield stress increases with increasing solids volume fraction for both ultra-fine calcium carbonate and barite samples. Calcium carbonate samples were stronger than the barite equivalents with yield stresses showing an increase of between 29% and 56%. Bailey et al. (1998) who performed filtration to completion with cake compaction and had yield stresses that were around 10 times higher than those presented here, also found that correspondingly

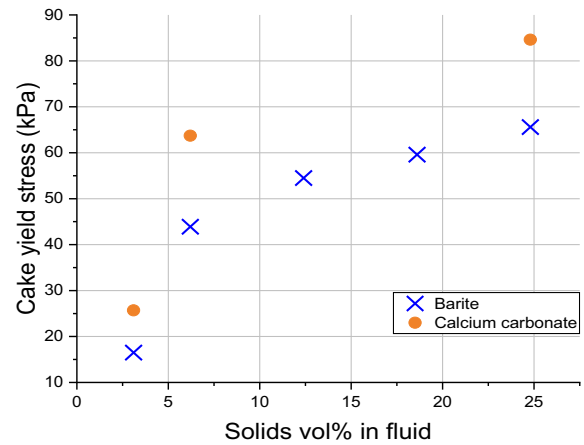


Fig. 6. Yield stress for cakes made from fluids with varying volume percentage of barite or calcium carbonate. Repeats were run for the sample with a barite loading of 6.2 vol% (SC2) and the standard error was 8%; error bars are not shown for clarity.

sized calcium carbonate filter cakes gave higher yield stresses than barite weighted filter cakes.

3.3. Varying particle shape

Particles of varying circularities were tested: glass spheres, calcium carbonate, barite, talc and cellulose microcrystalline. These particles were mixed into fluids at a constant volume fraction of 6.2 vol%. Apart from cellulose microcrystalline, these particles had similar median particle sizes (see Table 2 for d50 values and circularities).

Fig. 7 shows a plot of yield stress versus porosity for the filter cakes containing the various shaped particles. It is seen that cakes containing glass spheres and calcium carbonate (most circular) were strongest with yield stress values of around 64.0 kPa. These cakes also contained the highest filter cake solids fractions (lowest porosity); glass spheres produced the lowest porosity cakes out of all the samples tested at 0.34. Conversely, the less circular talc and cellulose microcrystalline particles produced filter cakes with high porosities of around 0.65. These filter cakes were also amongst the

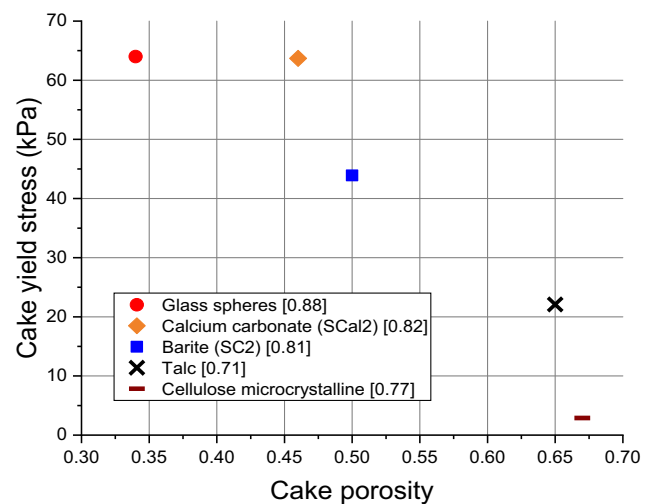


Fig. 7. Cake yield stress for cakes of different porosities, made from samples with varying particle shape; the number inside square brackets in the legend is the circularity of each particle.

weakest, with talc and cellulose microcrystalline cakes giving yield stress values of 22.1 kPa and 2.9 kPa, respectively.

3.4. Varying particle size distribution

The spans of the particle size distributions used were calculated using Equation (1) and plotted against yield stress as shown in Fig. 8. In Eq. (1), D_{10} , D_{50} and D_{90} are the particle sizes given by the intercepts for 10%, 50% and 90% of the cumulative volume of particles. Generally, filter cake yield stress increases as the span increases. However, DB3, which is composed of a combination of ultra-fine and coarse calcium carbonate, has the largest span at 12.8 but a significantly lower yield stress than is expected from the general trend. This trend may be due to a decrease in porosity as the span increases up to a span of 6 (Kinnarinen, Tuunila and Häkkinen, 2017), thereby increasing the interparticle contact surface area. Whilst for larger spans, as is the case with DB3, porosity has been found to increase with span (Peronius and Sweeting, 1985). The blended ratio (B1X and B2X) samples display opposite trends: the yield stress increases with span for the samples composed of 3.1 vol% barite, but, decreases as the span increases for the 6.2 vol% samples.

$$\text{Span} = \frac{D_{90} - D_{10}}{D_{50}} \quad (1)$$

4. Discussion

4.1. Yield stress and thickness

To understand how cake thickness and yield stress vary with filtration time, tests were performed on cakes produced over different filtration times of 5, 10, 15, 20 and 30 min. Samples SC2 (6.2 vol%) and SC5 (24.8 vol%) were chosen since, after 30 min of filtration, these samples produced cakes with a wide range of yield stresses, as shown in Fig. 6. In Fig. 9, the thickness of SC2 and SC5 cakes increased with filtration time. For SC2, both the measured peak force and the yield stress increase exponentially with filtration time and cake thickness. For SC5, there is an almost linear increase in both the measured peak force and yield stress with filtration time and cake thickness.

The relationship between cake yield stress and cake thickness for all samples tested is shown in Fig. 10. With low solids volume

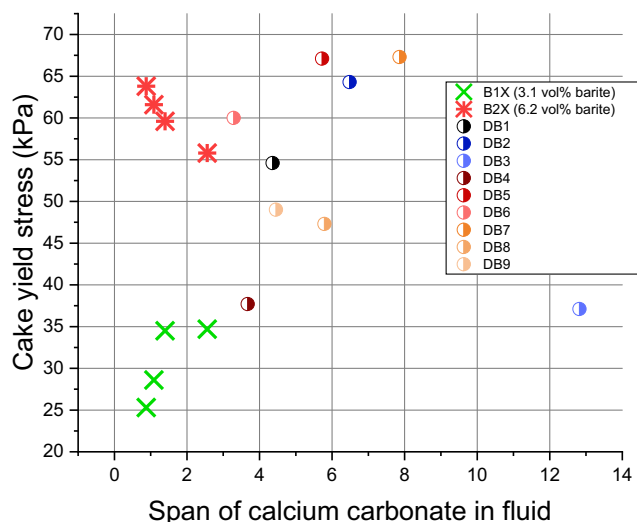


Fig. 8. Cake yield stress for cakes of different spans; the span of the calcium carbonate particles in the sample was used to create the graph.

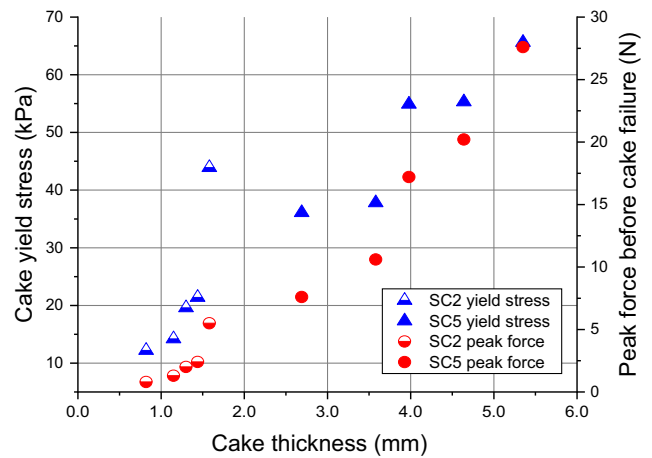


Fig. 9. Cake yield stress and peak force results for barite samples filtered for 5, 10, 15, 20 and 30 min which gives differing cake thicknesses. Repeats were run for SC2 filtered for 30 min and the standard error of the yield stress was 8%; error bars are not shown for clarity.

fraction in the fluid (SC1 and SC2), increasing the volume fraction increases the yield stress significantly. As expected, the cake thickness increases with solids volume fraction. Replacing the barite with an equivalent volume of calcium carbonate in the fluid produced filter cakes that are thicker, by between 0.50 and 0.93 mm, and are also stronger.

The addition of calcium carbonate particles of different sizes to the barite samples generally increased the cake yield stress. This could mean that the calcium carbonate is supplementing the core barite structure as shown in Fig. 11, whilst for two DB samples (DB3 and DB4), the calcium carbonate is having a detrimental effect. The DB samples are of similar thickness, yet the strongest cake, DB7, has a yield stress that is approximately double that of DB3, which may be due to DB7 having a lower porosity than DB3. Again, the blended ratio samples display opposite trends. As shown in the insert in Fig. 10, for samples with 3.1 vol% barite, the yield stress decreases as the blended ratio, and so the proportion of coarser particles, increases; for samples with 6.2 vol% barite, the yield stress increases as the blended ratio increases.

As was shown in Fig. 10, the calcium carbonate particles generally seem to be supplementing the core barite network, leading to

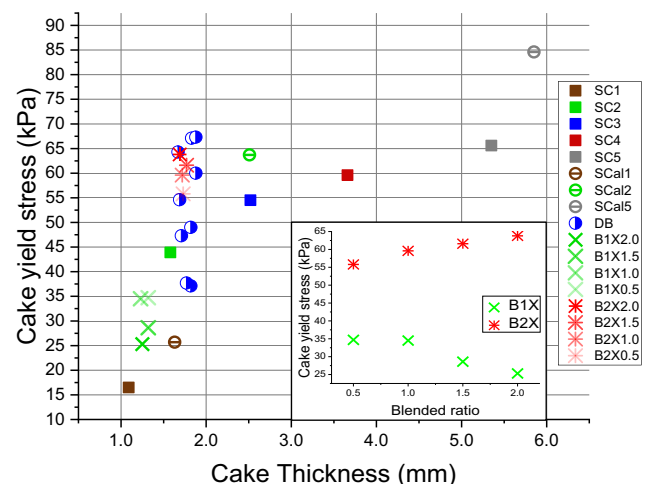


Fig. 10. Cake yield stress for cakes of different thicknesses. The insert shows the effect on yield stress as the blended ratio (the number after the 'X' in the sample name), and so the proportion of coarser particles, increases.

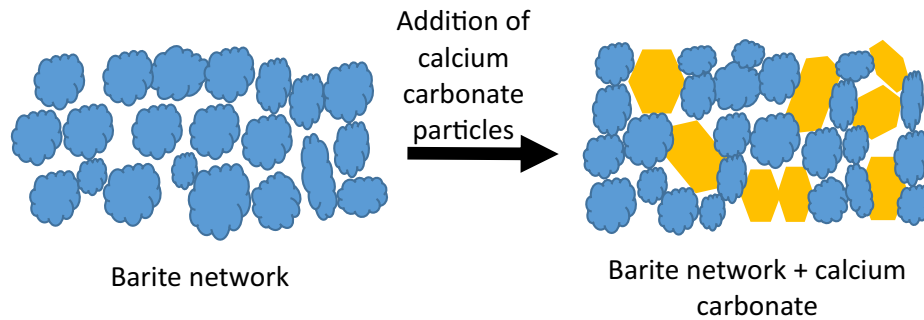


Fig. 11. Calcium carbonate particles supplementing the core barite network.

higher yield stresses for the samples that include both particles as opposed to barite only. The strength enhancement observed could be a result of either an increase in the interparticle contact surface area and/or a material property of calcium carbonate. It has been found for barite and calcium carbonate samples with a similar particle size distribution, the latter were observed to form filter cakes with significantly higher yield stresses (Bailey et al., 1998). From Fig. 6, a similar observation can be made as the calcium carbonate samples have yield stresses that are between 9.2 kPa (3.1 vol%) and 19.8 kPa (6.2 vol%) higher than the barite equivalents. It seems consistent that the increase in yield stress is more pronounced at the higher solids loading as more particle contacts will amplify any effects of increased cohesion between calcium carbonate particles. Also, the calcium carbonate only cakes are thicker (Fig. 10) and less porous (Fig. 12) than their barite only equivalents, hence will have a higher interparticle contact surface area. The yield stress is likely to be proportional to this surface area and so these cakes have a higher yield stress.

4.2. Yield stress and porosity

The relationship between cake yield stress and cake porosity for all samples tested is shown in Fig. 12. As porosity decreases, yield stress increases, with the cakes containing the various shaped particles giving the most extreme values. From Fig. 12, it can be seen that glass spheres give around the highest yield stress for the least porous cake; conversely, talc and microcrystalline cellulose give the lowest yield stresses with the highest porosities. The talc particles for instance have a plate-like shape (Bumiller et al., 2002)

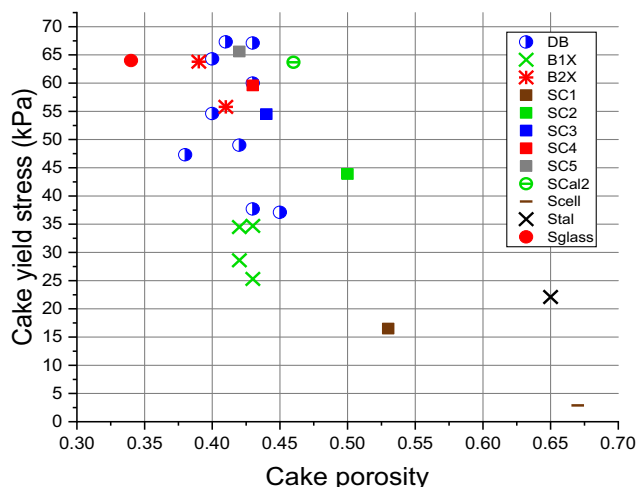


Fig. 12. Cake yield stress for cakes of different porosities.

and low circularity, and hence, may pack in sheet-like layers that are individually quite porous. Note that an arrangement of overlapping sheets may yet form a barrier of low permeability despite the filter cake's high porosity (due to the porous sheets). This sheet-like structure may be the reason for the low measured yield stress, because the resistance is derived from breaking these sheets as opposed to overcoming numerous particle contacts. Conversely, the high solids content glass sphere filter cakes gave a higher yield stress, presumably due to the high resistance required to restructure the tighter and more rigid packing structure.

As the barite volume fraction increases, the porosity decreases and the yield stress increases almost linearly. All the DB and B2X cakes have porosities that are between 0.08 and 0.14 lower than that of SC2, and, the B1X cakes have porosities that are between 0.10 and 0.14 lower than that of SC1. This reduction in cake porosity could be a consequence of the introduction of different particle sizes as calcium carbonate is added to the barite: the barite only samples (SC1 and SC2) have a span of 2.0, which is relatively low compared to the DB samples (Fig. 8). As a filter cake grows, fresh particles approaching the cake could either deposit on the cake's surface or within interstitial voids. When the homogeneous suspension being filtered consists of particles of a broad size distribution, this promotes the occurrence of the latter scenario whereby the finer particles in the distribution can migrate into pre-existing void spaces within the filter cake structure. This interstitial filling decreases porosity as the cake grows. Conversely, with a narrow size distribution, fewer particles are available which are fine enough to penetrate the filter cake's structure. Hence, filter cake growth will tend to involve a greater proportion of particles depositing on the cake's surface. This layered deposition will increase filter cake thickness more rapidly but has less of an impact on porosity. Both scenarios lead to an increase in total interparticle contact as the cake grows, and hence the cake's yield stress increases with filtration time (see Fig. 9 for example).

Furthermore, the data gathered suggests that a broad size distribution tends to give cakes with a higher yield stress (Fig. 8). Hence it may be postulated that the invasion of new particles into the filter cake structure followed by deposition within pre-existing voids is more beneficial to cake strength than a layered deposition mechanism. Intuitively, this could be due to two reasons: (a) particles depositing within pre-existing voids tend to form more contact points (per particle) compared to particles depositing on the cake's surface, and (b) the decreased void space surrounding particles make it more difficult for the structural rearrangements required during shearing. The preceding arguments are also consistent with Figs. 10 and 12 which show the DB filter cake samples to give similar thicknesses but a range of porosity and yield stress values. However, the DB3 sample, which is composed of ultra-fine and coarse calcium carbonate (in addition to barite), gave the largest span of the samples tested but also an unexpectedly low yield

stress. This apparent anomaly may be explained by the formation of segregated packing zones (non-homogeneous) within the filter cake when the size distribution is broad and concentrated at both ends of the distribution. In this case, the voids left behind by the coarse particles may be too large to effectively trap individual (or small clusters of) fine particles. This is analogous to the Brazil nut effect caused by vibrations in granular systems (Rosato et al., 1987), but in the case of filter cakes, it is caused by pressure-induced flow. It has been found that the Brazil nut segregation effect is strongest for mixtures with the largest particle size ratio (Liao, 2016) and the introduction of intermediate particle sizes have been found to reduce segregation of the particle mixture (Metzger et al., 2011).

5. Conclusions

Filter cakes made from different formulations were tested to assess the cake strength in relation to other cake properties and properties of the drilling fluid. Cake strength, measured as the yield stress, was improved by several factors. By increasing the barite solid loading in the drilling fluid from 3.1 vol% to 24.8 vol%, the cake yield stress increased from 16.5 kPa to 65.6 kPa. A similar trend was observed for cakes made from ultra-fine calcium carbonate. Furthermore, these cakes were stronger with yield stresses increasing by between 29% and 56% as compared to the barite equivalents. The increase in strength may be due to a higher interparticle contact surface area, which is a result of the calcium carbonate cakes being thicker and less porous than their barite equivalents. Fresh particles approaching the cake can either deposit on the cake's surface, increasing the cake's thickness, or within interstitial voids, decreasing the cake's porosity. A broad particle size distribution in the fluid encourages interstitial filling as finer particles migrate into pre-existing voids. Both scenarios lead to an increase in the total interparticle contact as the cake grows. However, broadening the particle size distribution in the cake tended to give stronger cakes of a similar thickness, as was illustrated by adding calcium carbonate of different sizes to barite-loaded fluids. Hence it was postulated that the deposition of new particles within pre-existing voids is more beneficial to cake strength than a layered deposition mechanism.

CRedit authorship contribution statement

Nikzad Falahati: Methodology, Validation, Formal analysis, Investigation, Writing - original draft, Visualization. **Alexander F. Routh:** Conceptualization, Formal analysis, Writing - review & editing, Supervision, Project administration, Funding acquisition. **Kuhan Chellappah:** Conceptualization, Writing - review & editing, Supervision, Project administration, Funding acquisition.

Declaration of Competing Interest

The authors declare that they have no known competing financial interests or personal relationships that could have appeared to influence the work reported in this paper.

Acknowledgements

The authors would like to acknowledge the funding and technical support from BP through the BP International Centre for

Advanced Materials (BP-ICAM) which made this research possible. The authors would like to thank Ian Collins (BP) and Giovanna Biscontin (University of Cambridge) for their advice, and Louise Bailey (Schlumberger) for her support with the hole punch test.

References

- Bailey, L. et al., 1998. Filtercake integrity and reservoir damage. In: SPE Formation Damage Control Conference. Society of Petroleum Engineers. <https://doi.org/10.2523/39429-MS>.
- Bumiller, M., Carson, J., Prescott, J., 2002. A preliminary investigation concerning the effect of particle shape on a powder's flow properties. In: World Congress on Particle Technology, pp. 21–25.
- Cerasi, P. et al., 2001. Measurement of the mechanical properties of filtercakes. In: SPE European Formation Damage Conference. Society of Petroleum Engineers. <https://doi.org/10.2118/68948-ms>.
- Chen, Y.S., Hsiau, S.S., 2009. Cake formation and growth in cake filtration. Powder Technol. 192 (2), 217–224. <https://doi.org/10.1016/j.powtec.2008.12.014>.
- Civan, F., 2015. Reservoir Formation Damage. Professional Publishing, Gulf.
- Cook, J. et al., 2016. The role of filtercake in wellbore strengthening. In: IADC/SPE Drilling Conference and Exhibition. <https://doi.org/10.2118/178799-MS>.
- Dewan, J.T., Chenevert, M.E., 2001. A model for filtration of water-base mud drilling: determination of mud cake parameters. *Petrophysics* 42 (3), 237–250.
- Fisher, K.A. et al., 2000. Numerical modelling of cake formation and fluid loss from non-Newtonian muds during drilling using eccentric/concentric drill strings with/without rotation. *Chem. Eng. Res. Design* 78 (July).
- Guo, Q. et al., 2014. A comprehensive experimental study on wellbore strengthening. In: IADC/SPE Drilling Conference and Exhibition. Society of Petroleum Engineers. <https://doi.org/10.2118/167957-MS>.
- Hall, L.D. et al., 2001. Magnetic resonance imaging for industrial process tomography. *J. Electr. Imag.* 10 (3), 601–607. <https://doi.org/10.1117/1.1377307>.
- Hao, H. et al., 2016. Comparative study on cementation of cement-mudcake interface with and without mud-cake-solidification-agents application in oil & gas wells. *J. Petrol. Sci. Eng.* 147, 143–153. <https://doi.org/10.1016/j.petrol.2016.05.014>.
- La Heij, E.J. et al., 1996. Determining porosity profiles during filtration and expression of sewage sludge by NMR imaging. *AIChE J.* 42 (4), 953–959. <https://doi.org/10.1002/aic.690420408>.
- Kinnarinen, T., Tuunila, R., Häkkinen, A., 2017. Reduction of the width of particle size distribution to improve pressure filtration properties of slurries. *Miner. Eng.* 102, 68–74. <https://doi.org/10.1016/j.mineng.2016.12.009>.
- Liao, C.C., 2016. Multisized immersed granular materials and bumpy base on the Brazil nut effect in a three-dimensional vertically vibrating granular bed. *Powder Technol.* 288, 151–156. <https://doi.org/10.1016/j.powtec.2015.10.054>.
- Metzger, M.J., Remy, B., Glasser, B.J., 2011. All the Brazil nuts are not on top: Vibration induced granular size segregation of binary, ternary and multi-sized mixtures. *Powder Technol.* 205 (1–3), 42–51. <https://doi.org/10.1016/j.powtec.2010.08.062>.
- Nandurdikar, N.S., Takach, N.E., Miska, S.Z., 2002. Chemically improved filter cakes for drilling wells. *J. Energy Resour. Technol.* 124 (4), 223–230. <https://doi.org/10.1115/1.1492841>.
- Peronius, N., Sweeting, T.J., 1985. On the correlation of minimum porosity with particle size distribution. *Powder Technol.* 42 (2), 113–121. [https://doi.org/10.1016/0032-5910\(85\)80043-7](https://doi.org/10.1016/0032-5910(85)80043-7).
- Rosato, A. et al., 1987. Why the Brazil nuts are on top: size segregation of particulate matter by shaking. *Phys. Rev. Lett.* 58 (10), 1038–1040. <https://doi.org/10.1103/PhysRevLett.58.1038>.
- Sedin, P., Johansson, C., Theliander, H., 2003. On the measurement and evaluation of pressure and solidosity in filtration. *Chem. Eng. Res. Design* 81 (10), 1393–1405. <https://doi.org/10.1205/026387603771339618>.
- Shen, C., Russel, W.B., Auzeais, F.M., 1994. Colloidal gel filtration: experiment and theory. *AIChE J.* 40 (11), 1876–1891. <https://doi.org/10.1002/aic.690401111>.
- Shirato, M. et al., 1971. Porosity variation in filter cake under constant-pressure filtration. *J. Chem. Eng. Jpn.* 4 (2), 172–177. <https://doi.org/10.1252/jcej.4.172>.
- Tan, C.P., Amanullah, M., 2001. Embedment modulus of mudcakes – its drilling engineering significance. In: AADE National Technology Conference & Exhibition, pp. 1–15.
- Tien, C., 2006. Introduction to Cake Filtration: Analyses, Experiments and Applications. Elsevier. <https://doi.org/10.1016/B978-044452156-9/50001-1>.
- Tiller, F.M., Hsyung, N.B., Cong, D.Z., 1995. Role of porosity in filtration: XII. Filtration with sedimentation. *AIChE J.* 41 (5), 1153–1164. <https://doi.org/10.1002/aic.690410511>.
- Zamora, M., Lai, D.T., Dzialowski, A.K., 1990. Innovative devices for testing drilling muds. *SPE Drill. Eng.* 5 (1), 11–16. <https://doi.org/10.2118/17240-pa>.